Rare Metal Materials and Engineering
Volume 53, Issue 8, August 2024
Available online at www.rmme.ac.cn

Science Press

Cite this article as: Zheng Ziqin, Huang Sizhu, Qu Wentao, et al. Electrochemical Corrosion, Wear, and Tribocorrosion Behavior of Novel Ti-19Zr-10Nb-1Fe Alloy[J]. Rare Metal Materials and Engineering, 2024, 53(08): 2137-2143. DOI: 10.12442/j.issn.1002-185X.20230693.

ARTICLE

Electrochemical Corrosion, Wear, and Tribocorrosion Behavior of Novel Ti-19Zr-10Nb-1Fe Alloy

Zheng Ziqin[1], Huang Sizhu[2], Qu Wentao[2], Wang Zhenguo[2,3]

[1] No. 52 Institute of China North Industry Group, Yantai 264003, China; [2] Mechanical Engineering College, Xi'an Shiyou University, Xi'an 710065, China; [3] Beijing Wanjie Medical Device Co., Ltd, Beijing 102609, China

Abstract: The electrochemical corrosion, wear, and tribocorrosion behavior of the novel Ti-19Zr-10Nb-1Fe alloy were investigated. The electrochemical corrosion analysis results show that the corrosion resistance of the Ti-19Zr-10Nb-1Fe alloy is better than that of the Ti-6Al-4V alloy under the test conditions in this research. Compared with the static electrochemical corrosion, the corrosion resistance of Ti-19Zr-10Nb-1Fe alloy during tribocorrosion decreases significantly, because the wear accelerates corrosion. The wear volume of Ti-19Zr-10Nb-1Fe alloy is increased with the increase in applied load whether the electrochemical corrosion occurs or not. Due to the acceleration effect of electrochemical corrosion, the wear volume caused by electrochemical corrosion is larger than that without electrochemical corrosion. The results of W_a/W_c are much greater than 10, indicating that during the tribocorrosion process, the material loss caused by mechanical wear is much larger than that caused by electrochemical corrosion. Through SEM observation of the wear morphologies of Ti-19Zr-10Nb-1Fe alloy after tribocorrosion, it can be inferred that the micro-abrasion is the main wear mechanism. The above results show that during the tribocorrosion process, the corrosion accelerates wear, and the wear accelerates corrosion.

Key words: electrochemical corrosion; wear; tribocorrosion; Ti-19Zr-10Nb-1Fe

Due to the presence of relative movements between bone and metal prosthesis and the corrosive effect of body fluids on the prosthesis, the service life of metal prostheses is severely affected[1]. Both wear and corrosion can cause great damage to the metal prosthesis, namely tribocorrosion process[2]. Consequently, wear debris and corrosion products are generated during tribocorrosion, which leads to osteolysis and prosthesis loosening, and eventually results in implant failure[3]. Hence, the tribocorrosion behavior of different biomedical metal materials, such as Ti-6Al-4V[2–5], CoCrMo[5], 316L stainless steel[6], Ti-20Zr-10Nb[7], Ti-24Nb-*x*Zr-*y*Sn[8], Ti-25Nb-3Mo-3Zr-2Sn[9], Ti-Nb-Ga[10], and pure Ti[11–12], has been investigated. Wang et al[7] studied the corrosion, wear, and tribocorrosion behavior of biomedical Ti-20Zr-10Nb alloy and found that the contribution of mechanical wear to the material loss of tribocorrosion is greater than that of corrosion. Salas et al[8] also mentioned that the abrasion is the main wear mechanism during tribocorrosion process.

Currently, titanium and titanium alloys are the most widely used medical materials because of their high specific strength, excellent wear resistance, corrosion durability, and biocompatibility[1,3–4,8]. New β type medical titanium alloys are composed of non-toxic elements, such as Nb, Ta, Zr, Fe, Mo, and Sn, and they have lower elastic modulus and higher strength[1,8–9,13–14]. Ti-19Zr-10Nb-1Fe alloy is one of the new β type medical titanium alloys[14]. The phase, microstructure, tensile strength, corrosion resistance, and biocompatibility of the Ti-19Zr-10Nb-1Fe alloy have been widely studied.

However, the tribocorrosion behavior of the Ti-19Zr-10Nb-1Fe alloy in the simulated body fluid has rarely been discussed. Thus, the effect of influence factors, such as abrasion, on the tribocorrosion behavior of Ti-19Zr-10Nb-1Fe alloy was investigated in this research. Besides, the electrochemical corrosion and wear behavior of Ti-19Zr-10Nb-1Fe alloy were also investigated.

1 Experiment

The Ti-19Zr-10Nb-1Fe (at%) alloy ingot of 100 g was

Received date: November 05, 2023
Foundation item: National Natural Science Foundation of China (52071261)
Corresponding author: Wang Zhenguo, Ph. D., Professor, Beijing Wanjie Medical Device Co., Ltd, Beijing 102609, P. R. China, E-mail: wzghappy@yeah.net

prepared through vacuum arc melting with non-consumable electrode, and the raw materials were high purity niobium (>99.9wt%), high purity iron (>99.9wt%), titanium sponges, and zirconium sponges. After melting in the WS-4 vacuum arc melting furnace, the water-cooled copper was used as the melting crucible. To ensure the composition uniformity of alloy, the ingot was smelted five times. Subsequently, the ingot was solution-treated in a box furnace at 900 °C for 6 h under the vacuum condition of 5×10^{-3} Pa followed by furnace cooling. Cube samples of 10 mm×10 mm×1 mm were used for electrochemical corrosion tests and the samples of 30 mm× 20 mm×2 mm were used for wear and tribocorrosion tests. The cube samples were ground and polished by SiC sandpaper (200#, 400#, 600#, 800#, 1000#, and 1200#) before tests. The density of the Ti-19Zr-10Nb-1Fe alloy is 5.72 g/cm^3.

CHI 660C potentiostat (CH, USA) equipment was used for the electrochemical corrosion tests with a standard three-electrode system. The Ti-19Zr-10Nb-1Fe alloy sample of 10 mm×10 mm×1 mm was used as the working electrode (WE), the reference electrode (RE) was a saturated calomel electrode (SCE), and the counter electrode (CE) was a platinum sheet electrode. During the electrochemical corrosion tests, the potential varied from −0.745 V to −0.195 V, and the scanning rate was 1 mV/s.

TE66 micro-abrasion tester (Phoenix Tribology, UK) was used for wear tests. The wear was performed under the conditions of sliding speed of 150 r/min (the rotation speed of ceramic ball), different loads (1.0, 2.0, 3.0, 4.0, and 5.0 N), and sliding distance of 47.9 m (600 r, rotation distance of ceramic ball). The ceramic ball with diameter of 25.4 mm was made of ZrO_2 and was used as friction pair. Al_2O_3 particles with size of 3.0±0.5 μm were selected as abrasive particles. The Hank's solution was used to simulate the physiological human body environment. The abrasive particle concentration was 0.01 g/cm^3.

TE66 micro-abrasion tester coupled with CHI 660C potentiostat was used for the tribocorrosion tests. During the tribocorrosion tests, the potential varied from −2.5 V to 1.0 V, and the corresponding scanning rate was 14.58 mV/s.

After wear and tribocorrosion tests, a calibrated digital optical microscope (OM, 15JE) was used to measure the diameter of the wear scar, and the worn surface was observed by scanning electron microscope (SEM).

The wear volumes of the material under different test conditions were calculated through Eq.(1)[7,9], as follows:

$$V=\pi b^4/64R \quad (1)$$

where V is the wear volume, b is the diameter of wear scar, and R is 25.4 mm (diameter of the ZrO_2 ceramic ball).

2 Results and Discussion

2.1 Electrochemical corrosion

The potentiodynamic polarization curves of the Ti-19Zr-10Nb-1Fe alloy are shown in Fig. 1. The corresponding corrosion potential (E_{corr}) and corrosion current density (i_{corr}) are determined by extrapolation as −0.533 V and 3.451×10^{-8} A/cm^2, respectively. Excellent corrosion resistance can be confirmed in the physiological medium. According to Ref. [14], the values of E_{corr} and i_{corr} are −0.668 V and 2.754×10^{-8} A/cm^2, respectively. The corrosion potential and corrosion current of relevant titanium alloys are listed in Table 1. It can be seen that the corrosion resistance of Ti-19Zr-10Nb-1Fe alloy is better than that of Ti-6Al-4V alloy, and the corrosion rate is also slower than that of Ti-20Zr-10Nb alloy. These results may be related to different alloying elements and phase composition. It is known that if the critical anodic current density is lower than 1.0×10^{-4} A/cm^2 for an active-passive metal in corrosion medium, the metal will be passivated spontaneously[14]. Hence, the Ti-19Zr-10Nb-1Fe alloy is likely to show a better passivation performance in the simulated body fluid.

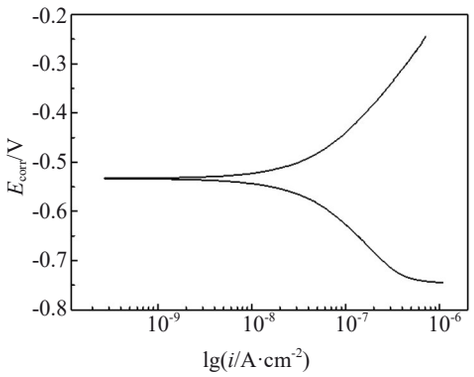

Fig.1 Polarization curves of Ti-19Zr-10Nb-1Fe alloy

Fig. 2 presents SEM morphology of Ti-19Zr-10Nb-1Fe alloy after electrochemical corrosion, and the pits on the surface cannot be observed, indicating the uniform corrosion. For metal implant materials, uniform corrosion is an important

Table 1 Corrosion potential (E_{corr}) and corrosion current density (i_{corr}) of different titanium alloys in Hank's solution

Alloy	E_{corr}/V	i_{corr}/A·cm^{-2}	Ref.
Ti-19Zr-10Nb-1Fe	−0.533	3.451×10^{-8}	-
Ti-19Zr-10Nb-1Fe	−0.668	2.754×10^{-8}	[11]
Ti-20Zr-10Nb	−0.457	1.089×10^{-7}	[7]
Ti-6Al-4V	−0.991	1.690×10^{-8}	[15]

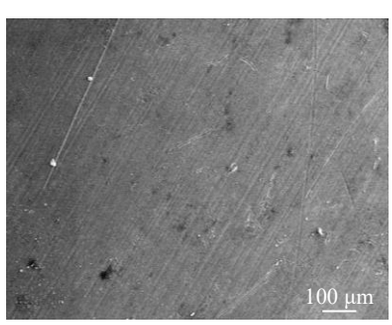

Fig.2 SEM morphology of Ti-19Zr-10Nb-1Fe alloy after electrochemical corrosion

property[16].

2.2 Wear

The wear volumes of Ti-19Zr-10Nb-1Fe alloy before electrochemical corrosion under different loads are shown in Fig. 3. It can be seen that the wear volume of Ti-19Zr-10Nb-1Fe alloy is increased with the increase in applied load, and this result is consistent with Archard's theory[4]. The wear volumes of Ti-19Zr-10Nb-1Fe alloy after wear with abrasive particles are larger than those without abrasive particles under the same test conditions, and the ratios of wear volume with abrasive particles to that without abrasive particles are 1.05–1.37. This is mainly because the wear is exacerbated by the abrasive particles in the Hank's solution, which can be trapped between the sample and the ceramic ball[17].

Fig. 4 shows the friction coefficients of Ti-19Zr-10Nb-1Fe alloy after wear without/with abrasive particles under different applied loads. The friction coefficients are basically decreased with the increase in applied load. When the applied load is lower than 3.0 N, the friction coefficient of Ti-19Zr-10Nb-1Fe alloy after wear without abrasive particles is larger than that with abrasive particles, and vice versa. Besides, the friction coefficients fluctuate greatly with the presence of abrasive particles under different load. Because of the existence of abrasive particles, the contact space between the ceramic ball and the sample becomes larger, and the movement and pulsation of particles are also intense[9].

Fig. 5 presents SEM morphologies of worn surface without and with abrasive particles at load of 2.0 N. All surfaces show classic ploughing phenomenon, which is caused by the hard ZrO_2 ceramic ball counter face, and the wear mechanism is typical abrasive wear. However, the width and depth of the plough furrow without abrasive particles are smaller than those of the plough furrow with abrasive particles. Apparently, there are large patches of wear products on the worn surface with abrasive particles, as shown in Fig. 5d. This is because the abrasive particles and the samples are crushed and pushed out by the ceramic ball[9,18].

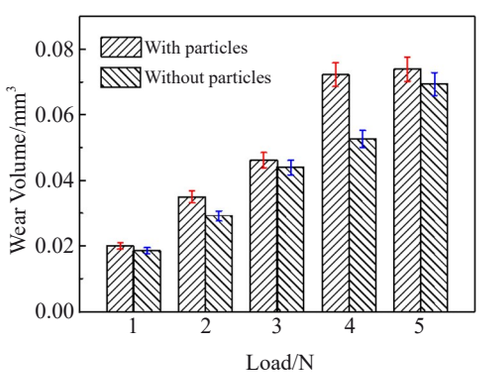

Fig.3 Wear volumes of Ti-19Zr-10Nb-1Fe alloy before electrochemical corrosion under different loads

2.3 Tribocorrosion

The typical dynamic polarization curves of Ti-19Zr-10Nb-1Fe alloy after wear without/with abrasive particles under different applied loads followed by tribocorrosion are presented in Fig. 6, and the corresponding corrosion potential and corrosion current density are listed in Table 2.

Compared with Fig. 1, the potential in Fig. 6 fluctuates, and the corrosion resistance of Ti-19Zr-10Nb-1Fe alloy during tribocorrosion decreases significantly. This is related to the actual surface degradation and this process can be described as a dynamic process of de-passivation and re-passivation[19]. Besides, the results also imply that the corrosion is accelerated by the wear during the tribocorrosion process.

The corrosion potential is basically decreased with the increase in applied loads. The results indicate that there is a large corrosion tendency under large applied loads. The range of corrosion potential is larger with abrasive particles, compared with that without abrasive particles. This is mainly because the presence of abrasive particles hinders the contact between the samples and the ceramic ball[6,20–21]. The friction fluctuates greatly. The corrosion currents are all at the order of magnitude of 10^{-5}, suggesting that the corrosion rates are similar even under different conditions.

The wear volumes of Ti-19Zr-10Nb-1Fe alloy after wear without/with abrasive particles followed by electrochemical corrosion are shown in Fig. 7. The results show that the wear volumes are increased with the increase in applied load, which agrees well with Archard's theory[4]. Obviously, the wear volumes with abrasive particles are larger than those without abrasive particles, and the ratios of wear volume with abrasive particles to that without abrasive particles are 1.23–1.59. This is mainly because the abrasive particles increase the

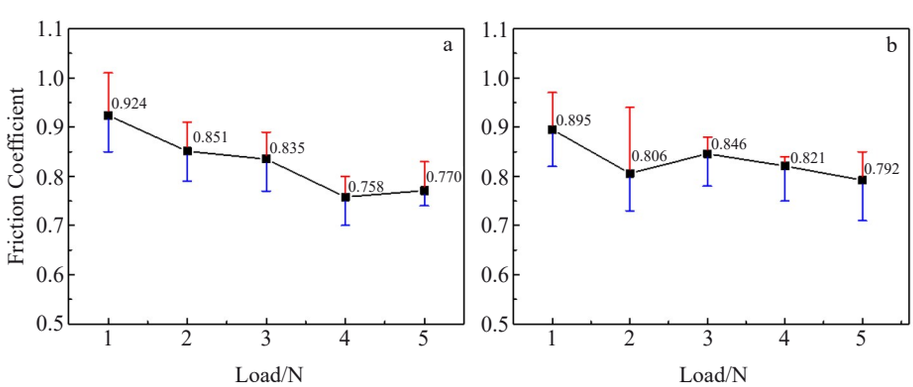

Fig.4 Friction coefficients of Ti-19Zr-10Nb-1Fe alloy after wear without (a) and with (b) abrasive particles before electrochemical corrosion

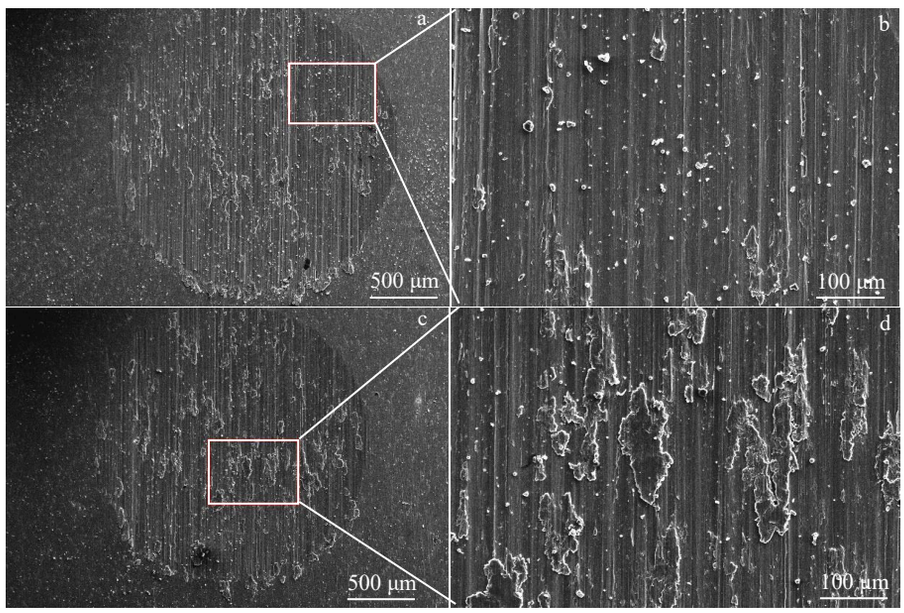

Fig.5 SEM morphologies of worn surfaces of Ti-19Zr-10Nb-1Fe alloy after wear without (a–b) and with (c–d) abrasive particles under load of 2.0 N

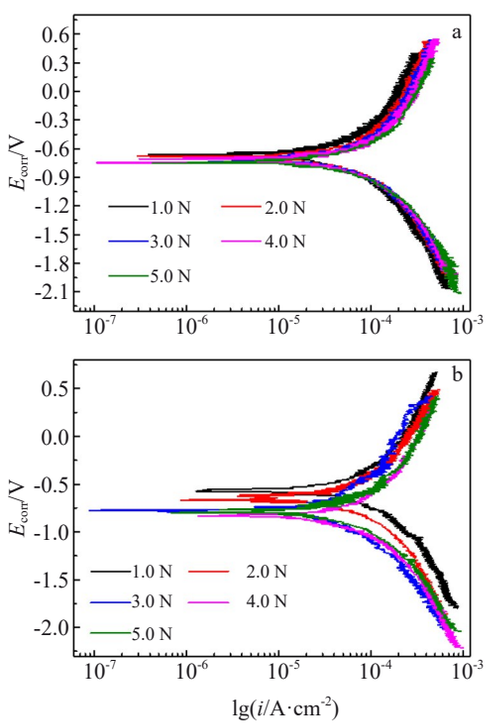

Fig.6 Polarization curves of Ti-19Zr-10Nb-1Fe alloy after wear without (a) and with (b) abrasive particles under different applied loads followed by tribocorrosion

Table 2 Corrosion potential (E_{corr}) and corrosion current density (i_{corr}) of Ti-19Zr-10Nb-1Fe alloy after wear without and with abrasive particles under different loads followed by tribocorrosion

Load/N	Without abrasive particles		With abrasive particles	
	E_{corr}/V	i_{corr}/×10^{-5} A·cm^{-2}	E_{corr}/V	i_{corr}/×10^{-5} A·cm^{-2}
1.0	−0.66	2.86	−0.56	2.66
2.0	−0.68	3.35	−0.66	2.65
3.0	−0.71	3.39	−0.77	1.86
4.0	−0.73	3.63	−0.83	2.19
5.0	−0.74	3.12	−0.78	2.28

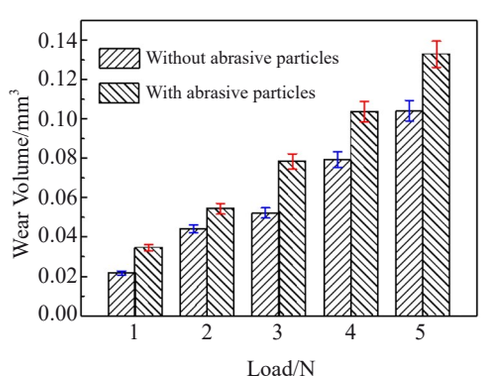

Fig.7 Wear volumes of Ti-19Zr-10Nb-1Fe alloy after wear without and with abrasive particles followed by electrochemical corrosion

destructive effect during the wear process. Besides, the wear resistance of Ti-19Zr-10Nb-1Fe alloy during tribocorrosion decreases significantly, and the electrochemical corrosion contributes to the material loss.

Compared with the results from Fig. 3, the wear volumes obviously increase after electrochemical corrosion, especially under higher loads. This result clearly shows that the electrochemical corrosion greatly degrades the material

property during the tribocorrosion process.

The corresponding friction coefficients are shown in Fig. 8. The friction coefficients obtained from the potentiodynamic tests are lower, compared with those of alloy before wear. This is mainly because of corrosion. The surface oxide film forms rapidly and serves as lubrication on the surface, leading to the significantly decreased friction coefficients[22–24].

SEM morphologies of worn surfaces of Ti-19Zr-10Nb-1Fe alloy after wear without/with abrasive particles under load of 5.0 N followed by tribocorrosion are shown in Fig. 9. It is evident that the typical wear mechanism is the three-body abrasion. Compared with Fig. 9b, more abrasive particles or wear products can be observed after the wear with abrasive particles (Fig.9d).

According to the wear volume, the total material loss (W_{ac}), which is caused by tribocorrosion, can be calculated through the density of Ti-19Zr-10Nb-1Fe alloy. Additionally, the W_{ac} can be divided into two parts, which are W_a and W_c, and its value can be calculated by Eq.(2)[9,24], as follows:

$$W_{ac}=W_a+W_c \quad (2)$$

where W_a is the total micro-abrasion loss and W_c is the corrosion loss calculated by Faraday's law based on the corrosion current density (i_{corr}). The values of W_{ac}, W_a, and W_c of Ti-19Zr-10Nb-1Fe alloy after tribocorrosion are listed in Table 3. In Ref. [25], when the $W_a/W_c>10$, the micro-abrasion is the main wear mechanism during the tribocorrosion process. According to the results in Table 3, the W_a/W_c ratios are much greater than 10, and the W_a/W_c ratios with abrasive particles are larger than those without abrasive particles. These results indicate that the micro-abrasion is the main wear mechanism, especially under the condition with abrasive particles.

Besides, it is also known that the material loss caused by corrosion is similar under all conditions, and the contribution of micro-abrasion to the material loss is the largest when the applied load is 5.0 N. The results show that the wear mechanism is dominant in tribocorrosion tests, compared with

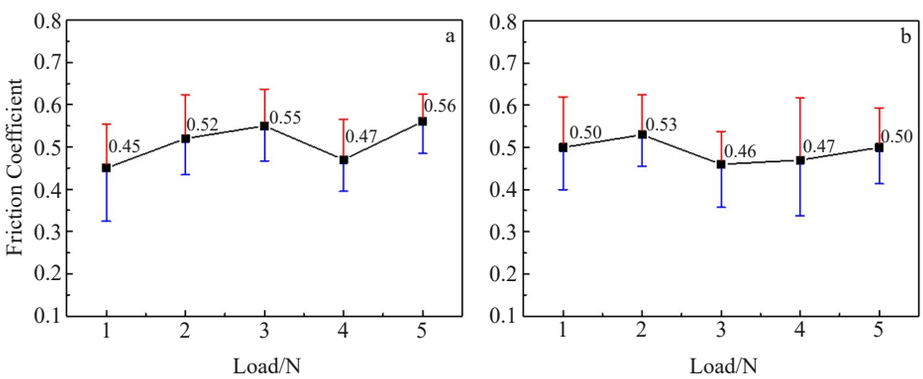

Fig.8 Friction coefficients of Ti-19Zr-10Nb-1Fe alloy after wear without (a) and with (b) abrasive particles followed by electrochemical corrosion

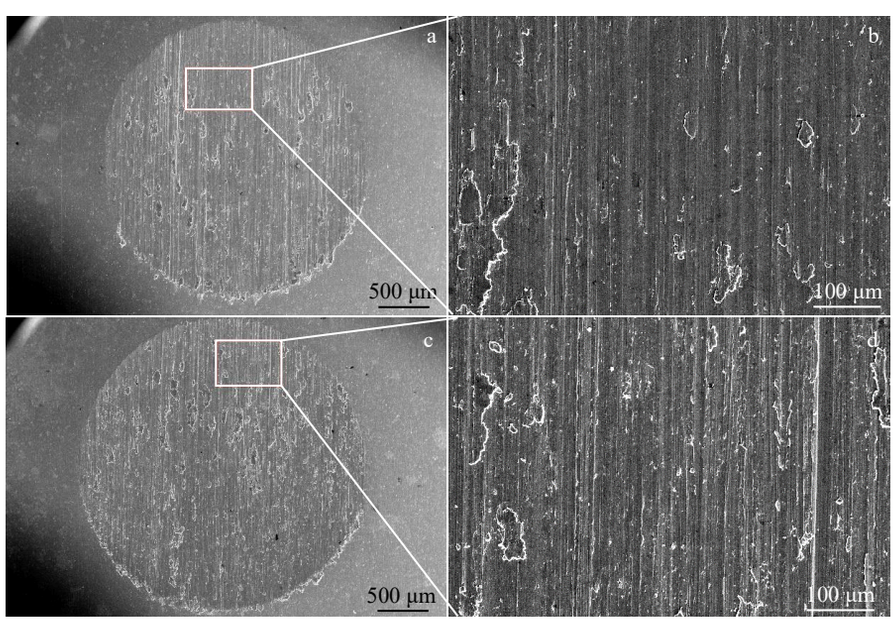

Fig.9 SEM morphologies of worn surfaces of Ti-19Zr-10Nb-1Fe alloy after wear without (a–b) and with (c–d) abrasive particles under load of 5.0 N followed by tribocorrosion

Table 3 W_{ac}, W_a, and W_c values of Ti-19Zr-10Nb-1Fe alloy after tribocorrosion

Load/N	Without abrasive particles				With abrasive particles			
	$W_{ac}/\times10^{-4}$ g	W_c/g	$W_a/\times10^{-4}$ g	W_a/W_c	$W_{ac}/\times10^{-4}$ g	W_c/g	$W_a/\times10^{-4}$ g	W_a/W_c
1.0	1.25	8.94×10^{-7}	1.24	138.84	1.98	1.01×10^{-6}	1.97	195.05
2.0	2.53	1.05×10^{-6}	2.52	240.63	3.11	1.00×10^{-6}	3.10	310.00
3.0	2.99	1.06×10^{-6}	2.98	281.19	4.48	7.04×10^{-7}	4.47	634.94
4.0	4.53	1.13×10^{-6}	4.52	398.27	5.93	8.29×10^{-7}	5.92	714.11
5.0	5.96	9.75×10^{-7}	5.95	610.18	7.60	8.63×10^{-7}	7.59	879.49

the corrosion mechanism.

The tribocorrosion contribution analysis for Ti-19Zr-10Nb-1Fe alloy (Table 3) clearly shows that total mechanical material loss (W_a and W_c) is the dominant material loss. However, W_a accounts for about 90% of the total material loss of Ti-19Zr-10Nb-1Fe alloy, presenting a direct response to the mechanical behavior of material. Briefly, the corrosion accelerates wear, and the wear also accelerates corrosion during the tribocorrosion process.

3 Conclusions

1) The corrosion resistance of Ti-19Zr-10Nb-1Fe alloy is better than that of Ti-6Al-4V alloy under the test conditions in this research.

2) Compared with that during the electrochemical corrosion, the corrosion resistance of Ti-19Zr-10Nb-1Fe alloy during tribocorrosion decreases more significantly. The wear volumes of the Ti-19Zr-10Nb-1Fe alloy are increased with the increase in applied load. The wear volumes are larger after electrochemical corrosion.

3) The micro-abrasion is the main wear mechanism. The corrosion accelerates wear, and the wear also accelerates corrosion during the tribocorrosion process.

References

1 Çaha I, Alves A C, Chiricoee C *et al. Corrosion Science*[J], 2020, 176: 108925

2 Sabeel M S, Abishek N R, Kurapati S S *et al. Materials Today: Proceedings*[J], 2021, 44(1): 157

3 Yazdi R, Ghasemi H M, Abedini M *et al. Applied Surface Science*[J], 2020, 518: 146048

4 Mohsen F, Khosro F, Mark T *et al. Tribology International*[J], 2022, 172: 107634

5 Righdan N, Rainforth W M. *Biotribology*[J], 2022, 30: 100212

6 Majdouline M, Itziar I A, Hicham B Y *et al. Materials Today: Proceedings*[J], 2022, 51(6): 1975

7 Fu T, Li H W, Wu F *et al. Rare Metal Materials and Engineering*[J], 2016, 45(5): 1128

8 Salas L, Chávez J, Jimenez O *et al. Materials Letters*[J], 2021, 283: 128903

9 Wang Z G, Huang W J, Li Y *et al. Materials Science and Engineering C*[J], 2017, 76: 1094

10 Ludovico A A, Jithin V, Yohan D *et al. Tribology International*[J], 2023, 181: 108325

11 Evangelos L, Owen R T T, Anna I M, *et al. Journal of the Mechanical Behavior of Biomedical Materials*[J], 2020, 102: 103511

12 Çiğdem A, İlyas H, Vangölü S Y *et al. Wear*[J], 2013, 302(1–2): 1642

13 Xue X D, Lu L B, Wang Z G *et al. Materials Letters*[J], 2021, 305: 130876

14 Xue P F, Li Y, Li K M *et al. Materials Science and Engineering C*[J], 2015, 50: 179

15 Wang Z, Huang W, Meng X. *Materials Science and Technology*[J], 2015, 31(11): 1335

16 Scharnweber D. *Encyclopedia of Materials: Science and Technology*[M]. New York: Elsevier, 2001: 555

17 Lin Cui, Zhao Licai. *Rare Metal Materials and Engineering*[J], 2013, 42(3): 507 (in Chinese)

18 Nan Rong, Li Silan. *Titanium Industry Progress*[J], 2022, 39(5): 28 (in Chinese)

19 Xu Y D, Qi J H, John N *et al. Tribology International*[J], 2021, 163: 107147

20 Mohsen F, Khosro F, Reza H. *Corrosion Science*[J] 2023, 215: 111047

21 Song Wei, Chen Qiang, Yu Shurong *et al*. *Rare Metal Materials and Engineering*[J], 2020, 49(7): 2393 (in Chinese)

22 Qi J, Guan D, Nutter J *et al. Acta Biomaterialia*[J], 2022, 141: 466

23 Lin B Z, Yang K H, Bao X G *et al. Journal of Non-crystalline Solids*[J], 2022, 576: 12123

24 Wang Yanfang, Lu Longqing, Xiao Lijun *et al*. *Rare Metal Materials and Engineering*[J], 2014, 43(2): 274 (in Chinese)

25 Wang Z G, Li Y, Huang W J *et al. Journal of the Mechanical Behavior of Biomedical Materials*[J] 2016, 63: 361

新型Ti-19Zr-10Nb-1Fe合金的电化学腐蚀、磨损和腐蚀磨损行为

郑自芹[1]，黄思著[2]，屈文涛[2]，王振国[2,3]

(1. 中国兵器工业第五二研究所烟台分所有限责任公司，山东 烟台 264003)

(2. 西安石油大学 机械工程学院，陕西 西安 710065)

(3. 北京万洁天元医疗器械股份有限公司，北京 102609)

摘 要：研究了新型Ti-19Zr-10Nb-1Fe合金的电化学腐蚀、磨损和腐蚀磨损行为。电化学腐蚀测试结果表明，在本研究实验条件下，Ti-19Zr-10Nb-1Fe合金的耐腐蚀性能优于Ti-6Al-4V合金。与静态电化学腐蚀相比，由于磨损加速腐蚀，在腐蚀磨损过程中Ti-19Zr-10Nb-1Fe合金的耐腐蚀性能明显降低。不论是否存在电化学腐蚀，Ti-19Zr-10Nb-1Fe合金的磨损体积随着加载载荷的增加而增加。由于电化学腐蚀的加速作用，Ti-19Zr-10Nb-1Fe合金磨损体积要大于无电化学腐蚀条件下的磨损体积。W_a/W_c结果远大于10，这说明在腐蚀磨损过程中机械磨损造成的材料流失远大于电化学腐蚀造成的材料流失。通过SEM观察Ti-19Zr-10Nb-1Fe合金腐蚀磨损后的磨损形貌可知，在腐蚀磨损过程中磨损占据主导作用。综合上述结果表明，Ti-19Zr-10Nb-1Fe合金在腐蚀磨损过程中，腐蚀加速磨损，磨损加速腐蚀。

关键词：电化学腐蚀；磨损；腐蚀磨损；Ti-19Zr-10Nb-1Fe

作者简介：郑自芹，男，1983年生，硕士，副研究员，中国兵器工业第五二研究所烟台分所有限责任公司，山东 烟台 264003，电话：0535-6891245，E-mail：zhengziqin111@163.com